Competition between radiative decay and energy relaxation of carriers in disordered $In_xGa_{1-x}As/GaAs$ quantum wells

M. Grassi Alessi, F. Fragano, A. Patanè, and M. Capizzi
Istituto Nazionale di Fisica della Materia, Dipartimento di Fisica, Università di Roma ''La Sapienza,'' Piazzale Aldo Moro 2, I-00185 Roma, Italy

E. Runge and R. Zimmermann
Humboldt-Universität zu Berlin, Institut für Physik, Hausvogteiplatz 5-7, D-10117 Berlin, Germany
(Received 13 April 1999; revised manuscript received 7 September 1999)

Photoluminescence (PL) and excitation PL measurements have been performed at different temperatures, excitation energies, and power densities in a number of strained $In_xGa_{1-x}As$ quantum wells where the fluctuations in the potential energy were comparable with the thermal energy. This has allowed us to observe a full series of anomalous temperature dependencies. These features, including some subtle ones, follow from the competition of thermalization and the degree of disorder in the samples. They are all accounted for by a theoretical model, which takes into account the excitons' radiative decay and phonon scattering in a disordered potential on an equal footing. Thus the interplay between finite lifetime and relaxation/thermalization is included in detail.

I. INTRODUCTION

The influence of morphological disorder on the optical properties of quantum wells (QW's) has been the subject of a number of theoretical and experimental papers in the last years. In heterostructures based on III-V semiconductors and their alloys, fluctuations in the well width and alloy composition modulate the local profile of the valence and conduction bands and strongly affect the optical properties. A number of theoretical and experimental groups have investigated, therefore, the dependence on the degree of disorder of the photoluminescence (PL) line shape, in particular of the full width at half maximum (FWHM) and of the ''Stokes shift'' (SS), i.e., the red shift of the QW PL emission with respect to the absorption.

The simulation of the competition between carrier thermalization and morphological disorder is somewhat simple in the two opposite limiting cases of very high or very low disorder, where the ratio ($\Delta = k_BT/W$) between the carrier thermal energy (k_BT) and the mean value of the disorder-induced potential fluctuations is a critical parameter. These fluctuations are probed by the value (W) of the FWHM of the heavy-hole exciton (HHE) band in photoluminescence excitation (PLE) spectra. In the limit of very high Δ (weakly disordered QW's and/or high T), the exciton thermal energy is higher than the difference between the local maxima and minima of the crystal potential, and the carriers are able to relax towards the absolute potential minimum. This holds even at low temperatures ($T = 5$ K) in the case of very weakly disordered systems. By assuming a Boltzmann distribution for the excitons and a Gaussian line shape for the exciton absorption, the Stokes shift turns out to be proportional to W^2/k_BT_c,[1] where T_c is the carrier temperature. In the opposite limit of low Δ (highly disordered samples and/or low T), the carriers relax towards local minima of the potential, whose stochastic distribution determines the peak energy of the free exciton emission and the value of SS. In the case of a Gaussian distribution for the local minima and of Gaussian spatial correlations, SS is given at zero temperature by $0.55W$.[2]

In recent years, the most general case of neither very strong nor very weak disorder has been studied systematically by two of the present authors (E.R., R.Z.).[3] In this case of ''intermediate'' disorder, the finite lifetime of excitons has to be taken into account. This introduces a competition between the radiative exciton decay and the exciton energy relaxation which is due to phonon scattering in the presence of local energy variations. It manifests itself in anomalous temperature dependencies: At low temperature, this competition leads to an incomplete relaxation of excitons, which are only partially thermalized, and to a nonmonotonic dependence on T of the Stokes shift. For increasing temperatures, SS increases until it reaches a maximum at T_M, then it decreases gradually as expected for an increasing carrier thermalization. Correspondingly, the PL HHE line shape narrows for increasing temperature, it reaches a minimum at T_m, then it broadens again at higher temperatures. A model describing excitons as classical particles performing a diffusive random walk in a disordered potential landscape leads also to quite similar results.[4] In this framework, the zero-T limit for the energy and shape of the PL band is quite different from that given by the theory of Ref. 2.

In the case of strained $In_xGa_{1-x}As/GaAs$ quantum wells, PL measurements have shown[5] that the thermalization and the localization models hold in the opposite limiting cases, respectively, of high and low temperatures—at least at low excitation power density. Both models fail, however, when a sizable fraction of carriers, but not all, are thermalized ($\Delta \approx 1$).[5] In this case, namely, in a large part of the (x, T) diagram of ternary alloys such as $In_xGa_{1-x}As/GaAs$ or other disordered systems, only a few reports on the effects of competition between carrier thermalization and potential well

fluctuations are found in the literature. Among them, a nonmonotonic dependence on T of the exciton PL peak energy E_p in InGaAs/InP single quantum wells has been attributed to exciton localization.[6] This behavior leads to a dip on the order of a few tenths of a meV in the dependence on T of E_p and to a minimum at finite T in the FWHM of the exciton PL band. Similar features have been observed in other III-V heterostructures, including InGaN,[7] both in QW's (Refs. 8–11) and in quantum dots.[12,13] Whenever noticed, these features have been ascribed to exciton localization effects, on the grounds of qualitative arguments. Finally, anomalous temperature dependencies also related to disorder have recently been observed[14] and theoretically discussed[15] on the basis of a classical hopping model assuming exponentially suppressed long-distance hops.

In this work, we perform a detailed analysis of the optical properties of a number of strained $In_xGa_{1-x}As/GaAs$ QW's as a function of temperature T and of exciting power density P. The use of samples grown by different techniques, with different indium concentrations and well widths, has allowed us (a) to observe a whole series of anomalous effects in the optical response of several samples with a different degree of disorder, (b) to relate those effects to the degree of disorder, and (c) to confirm all the main predictions of the model of Ref. 3 adapted to $In_xGa_{1-x}As/GaAs$ QW's. In particular, we provide evidence of the nonmonotonic, ''anomalous'' dependence on T of the Stokes shift and of the FWHM of the HHE band. We provide also a crude estimate of a shift toward high energy of the PLE emission with respect to the HHE absorption. This shift is induced by disorder, as thoroughly discussed in the theory section, and provides evidence of an effective mobility edge for exciton relaxation near the center of the excitonic absorption. Finally, a detailed comparison of simulation results for the relaxation kinetics with experimental results is presented.

II. THEORETICAL APPROACH

We present a microscopic treatment of the effects of disorder on the basis of the model of Ref. 3. Therein, the effective potential relevant for exciton localization is determined by the strength of the disorder and the internal exciton wave function, which in turn is determined by material parameters. We briefly summarize the method and the choice of the parameter values entering the model. Under quite general circumstances, the effect of the disorder on the *relative* motion of electron and hole can be neglected in comparison with its influence on the center of mass motion of the exciton as an entity. The center of mass eigenstates satisfy a single-particle Schrödinger equation with a spatially correlated potential. In a given computer-generated disorder realization, the exact disorder eigenstates are determined. The matrix elements of the deformation potential scattering operator and the radiative coupling to the light field yield the state-dependent rates for exciton recombination and relaxation, which determine the spectra observed in the different optical experiments (PL, PLE, absorption, etc.) We use whenever possible the values and interpolation formulas of Ref. 16. Besides the parameter values reported in Table I, we use the usual ratio of 2:1 (only very inaccurately known) for the band offset and the value of 13.9 (14.6) for the $In_xGa_{1-x}As$ dielectric constant in the case $x=0.5$ (0.8). Image potential effects for a barrier dielectric constant of 12.5 are included in the determination of the exciton relative wave function.[17] The prefactor of the radiative decay rate is found to be close to that of GaAs/AlGaAs system, thus we use $\gamma_{\rm rad}/|\Psi_{Q=0}|^2=10^{-5}$ nm^{-2} ps^{-1} as in Ref. 3. The acoustic phonons are assumed to be those of GaAs with sound velocity $\hbar\nu=3.3$ meV nm and stiffness $c_{11}=\nu^2\rho=5.1$ meV nm^{-3}. A general agreement is found in the literature on the basic effect that radiation and exciton-phonon interaction determine the low-excitation luminescence. On the contrary, not much is known for certain input parameters, in particular the deformation potentials for the individual bands, as opposed to the difference between valence and conduction band contributions. The latter difference is the only easily accessible parameter and is experimentally determined by optical measurements under hydrostatic pressure. It is then linearly interpolated between the values it has in GaAs and InAs

TABLE I. Exciton parameters entering the theoretical estimates of the Stokes shift and FWHM for the HHE PL band as a function of T for the different samples investigated in the present work: Bohr radius a_B, binding energy E_B, electron (e) and heavy-hole (hh) effective masses in units of the free electron mass m_0.

Sample	a_B (nm)	E_B (meV)	$m_e(m_0)$	m_{hh} (m_0)
A, D	12.3	9.6	0.061	0.174
B	12.4	8.8	0.065	0.18
C	11.3	9.9	0.056	0.16

$$D_c-D_v=(-8.4+2.4x)\ \text{eV}. \tag{1}$$

Since the *individual* values of the deformation potential are needed in our simulations, we have run our simulations for two different choices of the ratio $R=D_v/D_c$. The trial values of R are 0.1, as its best estimate for GaAs,[18] or a much larger value, 1.

The in-plane heavy-hole masses of Table I are determined from a four-band $\mathbf{k}\cdot\mathbf{p}$ calculation with Luttinger's γ-parameters obtained from a quadratic interpolation of those in Ref. 19. A strain induced heavy-light hole splitting of 0.42 eV is used.[16] The electron mass of the well material is extrapolated from a figure in Ref. 16 and a weighted average of barrier and well mass is used; see Table I. Finally, the exciton kinetic mass is given by the sum of the electron and heavy-hole masses, $M=m_e+m_{hh}$. However, it should be warned that $\mathbf{k}\cdot\mathbf{p}$ theories are not accurate for thin wells such as the ones under consideration. In particular, for the parameter set used, no confined light-hole single particle state is found in the well region. This would imply that the light-hole exciton is of type II character. For thin wells, as in the present case, the electron wave function penetrates deeply into the barrier and such a type II exciton has an oscillator strength comparable to those of, e.g., the GaAs/GaAlAs type I excitons. The energetic position of type II excitons in these cases is, therefore, determined mostly by the electron confinement. As a matter of fact, well pronounced light-hole exciton recombinations appear in Fig. 1 at energies not much above those of the corresponding

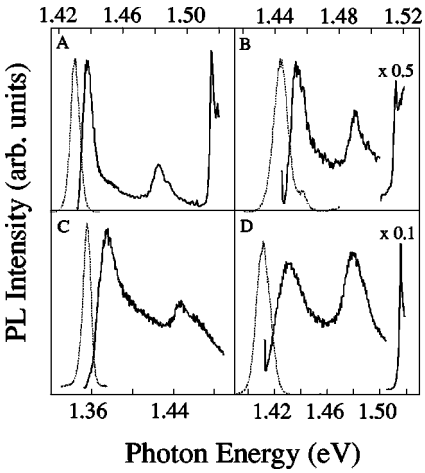

FIG. 1. PL (dotted line) and PLE (full line) spectra at $T=10$ K for samples A, B, C, and D. The PL spectra exhibit a single band which is related to heavy-hole exciton recombination. In the PLE spectra, the peaks of heavy- and light-hole excitons, and that of the GaAs barrier free exciton are observed with increasing energies.

heavy-hole excitons. These features are consistent with the predicted type II character for the light-hole excitons.

In the next step, exciton Bohr radii and binding energies are determined with a variational ansatz for the relative exciton wave function including the image charge interaction. The Bohr radius is needed for the calculation of the effective potential for the center of mass motion. With the assumption of a short range disorder, the whole approach involves only a single parameter, which is adjusted to the specific sample. This parameter is the strength σ of the local energy variations. It is determined by fitting the width of PL or PLE bands. Typically, σ is about 1–1.5 W. Note, that both PL or PLE bandwidth and σ are considerably less than the underlying energy variations due to, e.g., local monolayer fluctuations which are of the order of 100 meV for our case.[20,21] This can be understood as motional narrowing: As an extended object, the exciton averages over the underlying potential fluctuations. For given σ, a numerical solution of the Schrödinger equation yields the wave functions and thus absorption spectra. PL and PLE spectra follow from subsequently solving the kinetic equation for exciton relaxation given in Ref. 3.

III. EXPERIMENTAL RESULTS AND COMPARISON WITH THEORETICAL SIMULATIONS

A. Experimental details

In order to investigate samples with different degrees of disorder, PL measurements have been carried out on four $In_xGa_{1-x}As/GaAs$ QW's with different values of indium concentration x (0.5 or 0.8) and well width L (from 2 to 7 monolayers, ML); see Table II. [22,23] For the same reasons, PL and PLE measurements were performed at temperatures ranging from 4.2 to 100 K. Three samples (A, B, and C) have been grown by molecular beam epitaxy (MBE) at 460 °C, one (D) by metal organic chemical vapor deposition (MOCVD) at 520 °C. The excitation sources were either an Ar^+ laser or a Ti:sapphire tunable laser. The PL emission, excited by the 488 nm line of the Ar^+ laser or the 770 nm line of the Ti:sapphire laser, was dispersed by an asymmetric DMS-2 SOPRA double monochromator with an equivalent focal length of 75 cm and detected by standard photon counting techniques. Emission bands have been fitted by Gaussian line shapes in order to better define the peak energies.

TABLE II. Nominal indium concentration x, well thickness L, growth method, and growth temperature T_G, for the $In_xGa_{1-x}As$ samples investigated in the present work. The values W of the FWHM measured at 10 K in PLE for the HHE band, an index of the degree of disorder in the samples, are reported in the last column. Estimates of the relative uncertainties in the values of x and W are also given.

Sample	x	L (ML)	Growth	T_G (°C)	W (meV)
A	$0.5\pm10\%$	4	MBE	460	$9.0\pm5\%$
B	$0.8\pm5\%$	2	MBE	460	$12.0\pm5\%$
C	$0.5\pm10\%$	7	MBE	460	$17.5\pm5\%$
D	$0.5\pm5\%$	4	MOCVD	520	$25.5\pm5\%$

B. Stokes shift

The PL and PLE spectra taken at 10 K for the $In_xGa_{1-x}As/GaAs$ samples reported in Table II are shown in Fig. 1.[24] All measurements reported in this paper unless otherwise noticed have been performed in a linear regime—the exciton line shapes did not change for excitation intensities varying by roughly three orders of magnitude. The detection energy in the PLE spectra has been choosen on the low energy tail of the PL band in order to optimize the observation of the HHE band. The FWHM of the heavy-hole exciton increases on going from sample A to sample D, both in the PL and PLE spectra, which corresponds to an increase in the degree of disorder. In the PLE spectrum of sample A, grown by MBE, the HHE signal is three times higher than that of LHE and comparable with that of the GaAs free exciton, as usually found in not too disordered QW's. In the PLE spectrum of sample D, with a higher degree of disorder, the HHE signal is comparable to that of LHE.

In Fig. 1, the HHE and LHE signals in sample D are ten times smaller than that of the GaAs free exciton. A reduction of the QW signal with respect to the one of the GaAs barrier has been observed in strongly disordered heterostructures where it has been attributed to the presence of a mobility edge for relaxation.[25] This feature gives rise to a suppression of exciton relaxation into low-energy states and to an asymmetric decrease of the HHE contribution to the PLE spectra compared to the case of perfect thermalization. The presence of a mobility edge also leads to a dependence of the PLE spectra on detection energy E_{det} as shown in Fig. 2 in the case of sample C. A clear change in the PLE spectra can be observed for E_{det} going from the high to the low-energy side of the PL band, reported in the figure for sake of comparison. The weight of the HHE band relative to the exciton continuum suddenly decreases for $E_{det}\lesssim1.360$ eV, the most likely value for the relaxation mobility edge in this sample. Also the peak energy of the PLE band shows a tiny dependence on the detection energy and shifts by ≈1 meV toward higher energies for decreasing detection energies.

The discussion of the effect of disorder on the optical properties of a $In_xGa_{1-x}As/GaAs$ QW will be focused on the

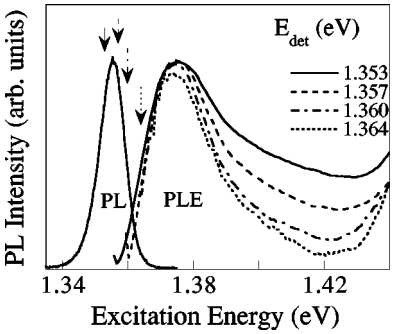

FIG. 2. PLE spectra at 10 K of the heavy-hole exciton in sample C for different detection energies indicated by arrows and normalized to maximum. The PL spectrum at 10 K is also shown for comparison.

dependence on temperature and exciting-power density of the Stokes shift, a clear probe of the presence of a mobility edge in QW's, and of the FWHM of the HHE band observed in PL spectra. This discussion will be performed initially in the case of sample C, which exhibits an intermediate degree of disorder with respect to the other samples investigated here; later it will be extended to the other samples.

The Stokes shift is usually defined as the difference between the peak energies of the HHE bands in the absorption and PL spectra. The determination of the absorption spectra of thin QW's requires the removal by chemical etching of the substrate. This procedure is unsuitable in the case of strained QW's such as those investigated here since it leads to a change in the strain—and, therefore, in the optical response—of the investigated sample. In the case of strained QW's SS is commonly estimated as the the difference between the HHE peak energies in PLE and PL spectra, the former being equated approximately to absorption spectra. In turn, this estimate of SS can be easily compared with that obtained from numerical simulations of PL and PLE spectra as those reported in the following theory section. It should be mentioned, however, that the slight dependence of the PLE spectra on detection energy reported in Fig. 2 introduces an uncertainty of the order of 1 meV in the estimate of SS from PLE spectra.

The peak energies of the HHE bands in the PL and PLE spectra of sample C are reported in Fig. 3 as measured at different temperatures. They provide the dependence on T of the Stokes shift, which is indicated at 10 K by the double-headed arrow in the figure. The PLE peak energy (diamonds) decreases with increasing T, roughly following the InGaAs

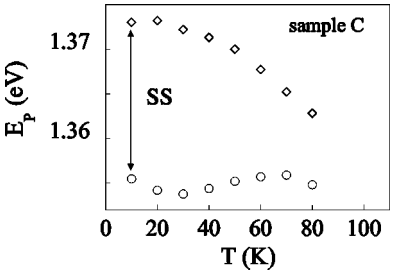

FIG. 3. Temperature dependence of the PL (circles) and PLE (diamonds) heavy-hole exciton energy peaks E_p for sample C. The PL Stokes shift (SS) at 10 K is displayed by a double-headed arrow.

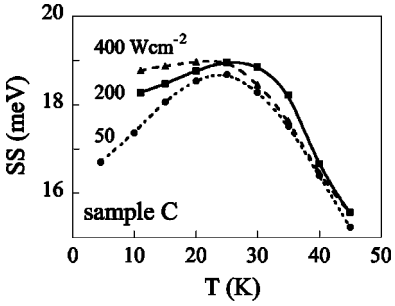

FIG. 4. Temperature dependence of the Stokes shift in sample C for different excitation power densities. The lines are guides to the eye.

energy gap. On the contrary, the dependence on T of the PL peak energy (circles) exhibits a sigmoid, nonmonotonic behavior which leads to the corresponding nonmonotonic dependence on T of the Stokes shift reported in Fig. 4. Therein, for a fixed exciting power density SS goes through a maximum at a temperature $T_M \neq 0$ which justifies the term ''anomalous'' Stokes shift commonly used in the literature. In the framework of any thermalization model SS decreases monotonously for increasing carrier temperature, e.g., proportional to $W^2/k_B T_c$. Since the PL emission intensity linearly increases on an extended range of power densities ($0.5\ \mathrm{W\,cm^{-2}} \leqslant P \leqslant 500\ \mathrm{W\,cm^{-2}}$), as expected in quasi-2D system, the dependence of T_M on P displayed in Fig. 4 further supports a tight correlation between the ''anomalous'' SS and exciton thermalization effects in a disordered potential. In fact, the ''anomalous'' dependence of SS on T is monotonously smeared out for increasing P when excitons increasingly fill the potential local minima until they thermalize again in an ordered ''effective'' potential. For similar reasons SS tends monotonously to zero at higher Ts where its value is roughly independent of P, as shown in the figure. It should be noticed that the dependence of SS on P is maximum at the lowest T, which provides a further contribution to the experimental uncertainty in the estimate of SS.

In the same temperature range where SS goes through an ''anomalous'' maximum, the FWHM of the HHE band in PL goes through an equally ''anomalous'' minimum, as shown in Fig. 5(a), at a temperature $T_m \neq T_M$. This effect is more

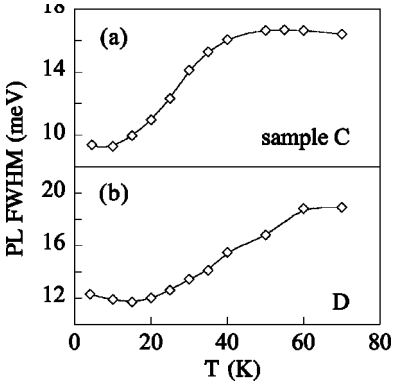

FIG. 5. Temperature dependence of the FWHM of the HHE PL band for (a) sample C and (b) sample D. The full lines are guides to the eye.

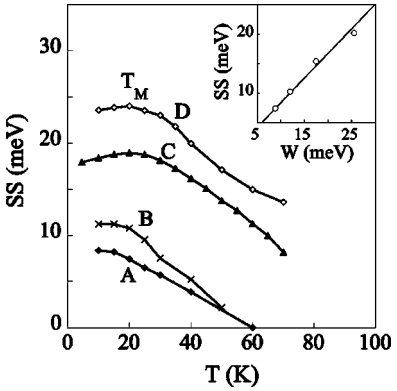

FIG. 6. Temperature dependence of the Stokes shift for all the $In_xGa_{1-x}As$ samples studied in the present work. The values of the Stokes shift at 10 K are reported in the inset as a function of *W*, the FWHM of the heavy-hole exciton band in PLE spectra. The full lines are guides to the eye.

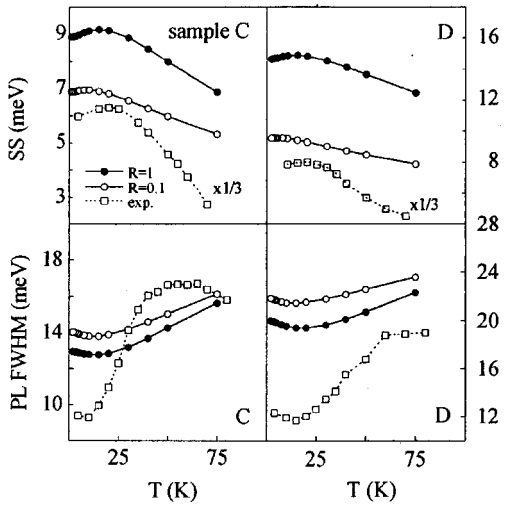

FIG. 7. Simulation results for parameters corresponding to samples C (left) and D (right). Room temperature PLE-FWHM are 19 and 29 meV, respectively. The shift SS of the PLE maximum at 10 K relative to the peak positions of the HHE band in the PL is reported in the upper panels as a function of *T*. The FWHM based on moments of PL histograms obtained for luminescence at different temperatures is shown in the lower panels. Full lines through open circles (solid dots) are guides to the eyes for simulations obtained by using a D_v/D_c ratio of 0.1 (1). The experimental data reported in Figs. 5 and 6 for samples C and D are also shown for sake of comparison by open squares (scaled by 1/3 in the case of SS). Note the differences in the minima and maxima positions, which are addressed in the text in detail.

evident in the case of the more disordered sample D, where the minimum in FWHM vs *T* is deeper and at higher temperature; see Fig. 5(b).

These temperature dependencies can be qualitatively explained in the framework of exciton localization in potential energy relative minima. For temperature increasing from $T=0$, excitons begin to thermalize and relax to the absolute potential minimum. Therefore, the PL HHE peak energy shifts towards lower energy, SS increases, and the FWHM decreases. Then, as the temperature increases further, the exciton population starts to spread over the full density of states. The FWHM begins to increase, while the PL shifts toward higher energies, and SS decreases.

For an increasing degree of disorder in the samples, namely, on going from sample A to sample D, all the properties reported for sample C and attributed to disorder change accordingly: T_m, SS, and T_M increase, indeed, with *W*. This has already been shown in Fig. 5 for T_m. The values of the Stokes shift, determined for all samples as done for samples C, are reported as a function of temperature in Fig. 6. In all samples SS has an ''anomalous'' temperature dependences with a T_M which is higher and better defined the more disordered is the sample. In the case of the least disordered sample A, T_M is smaller than 4.2 K, at least in the limit of our experimental energy resolution (0.1 meV). Finally, at all temperatures SS increases with the degree of disorder *W*. At 10 K, SS depends linearly on *W* with a slope equal to 0.8 (full line in the inset), quite higher than that predicted (0.55) in Ref. 2 for a fully disordered system. It may be worth noticing that T_m's on the order of 150–200 K have recently been reported for the emission bands of self assembled quantum dots in InGaAs/AlGaAs heterostructures. In that case, those anomalies have been attributed to carrier hopping between dots which is expected to give rise to a behavior similar to that predicted in highly disordered QWs.[13]

Simulation results obtained on the basis of the model described in the theory section are reported in Fig. 7. Here, the PL FWHM (lower panels) and the Stokes shifts (higher panels) corresponding to those experimentally determined in the previous section for samples C and D have been displayed as a function of *T*. The corresponding experimental data (open squares) are also displayed for comparison's sake. These simulations have been obtained for a choice of parameters corresponding to those of the two more disordered samples C and D (left and right panels, respectively). Full lines refer to simulations for $R=D_v/D_c=1$, dashed lines to simulations for $R=0.1$. The only free parameter entering the simulations is the degree of disorder which is reflected in the value of *W*, the high-temperature PLE FWHM. We used disorder strengths such that the room temperature values of *W* are 19 and 29 meV for samples C and D, respectively. The value of *W* at low *T* is slightly less, due to the effect of an incomplete thermalization. For both values of *R* the simulations only qualitatively reproduce the nonmonotonic behavior experimentally found for SS and the PL FWHM. Also the characteristic temperatures T_m and T_M approximatively agree with their experimental counterparts estimated at the lowest possible *P*. However, the relative positions of T_m and T_M differ both from the experiments and from what has been found for the GaAs simulations.[3] This shows that details matter in the simulations and that the nonmonotonic behavior cannot universally be rescaled from one sample to the other. It should be emphasized again that the semiquantitative agreement on existence and position of minima in PL position and linewidth is possible only due to the inclusion of both energy relaxing and radiative processes and to the kinetic description resulting in a nonthermal distribution. Two features regarding the remaining quantitative deviations between experiment and theory in Fig. 7 are noteworthy.

(i) The quantitative agreement with the experiment is fair for $R=0.1$, it improves for $R=1$. Higher values of *R* would be better but, as stated above, there is no independent data on the deformation potential ratio *R* for InGaAs QW, which is a

strained system. Furthermore, we cannot exclude that part of the residual discrepancies with the experimental results may come from details in the confinement wave functions at the interfaces and other small differences. In particular, the temperature dependence of the Stokes shift and the PL FWHM depend sensitively on the ratio between the radiative lifetime and the phonon scattering time at the different energies. The latter depends on the deformation potentials (and on R), among others, which enter roughly in the combination

$$\gamma_{\text{phonon}} \sim \left[D_c \chi\left(\frac{m_h}{M} q_\parallel\right) - D_v \chi\left(\frac{m_e}{M} q_\parallel\right) \right]^2 \qquad (2)$$

with $\chi(q)$ being the Fourier transform of the squared exciton wave function for the relative motion of electron and hole. The momentum transfer q is determined by the energy difference. As $\chi(q)$ falls rapidly from unity with increasing argument, the phonon scattering is much larger if the smaller mass goes along with the larger fraction of the total deformation potential than in the opposite case. Higher values of R correspond therefore to higher values of γ_{phonon} and faster relaxation. One could speculate that in disordered QW's the electron-phonon coupling increases compared to the perfectly ordered bulk case, e.g., because of confinement effects and of abrupt lattice changes at the interfaces.

(ii) Variations with temperature are stronger in the experimental data than in the simulations. This rules out certain possible sources of systematic experimental errors such as a long-range inhomogeneous broadening. It suggests that our theory slightly underestimates energy relaxation or overestimates the rate of radiative decay. One possible origin of the former possibility, the insufficient knowledge of deformation potentials, has already been discussed. Involvement of other phonon branches (optical phonons) is another possibility.

Assumption of longer lifetimes would also favor stronger ''anomalous'' behavior and bring theoretical results closer to the experiments. We do not show such calculations because, in contrast to the phonon scattering, there is not much uncertainty in the choice input parameters for the calculation of radiative lifetimes. However, there are many examples of low-dimensional semiconductor systems where experimental radiative lifetimes and theoretical predictions disagree. Generally, in these cases, the latter is too short, as it might be in the present case as well.

At the moment, the only sample-specific input parameter is the disorder strength W, which, from its very definition, cannot be predicted independently. *Ad hoc* assumption of a longer radiative lifetime would be in conflict with this first-principle character of the theory.

C. Other effects related to disorder

Fluctuations in the potential energy may lead to other nontrivial effects in the optical properties of disordered QW's. In Fig. 8, we present simulation results for the PL (higher panel) and PLE spectra (lower panel) of the HHE band in sample C at different temperatures. The simulation for the absorption spectrum is also shown in both panels. These simulations have been obtained by smooth fits through histograms of data in the $R=1$ case. Since the PLE line shape weakly depends on detection energy, as experimentally found and reported in Fig. 2, the displayed PLE curves

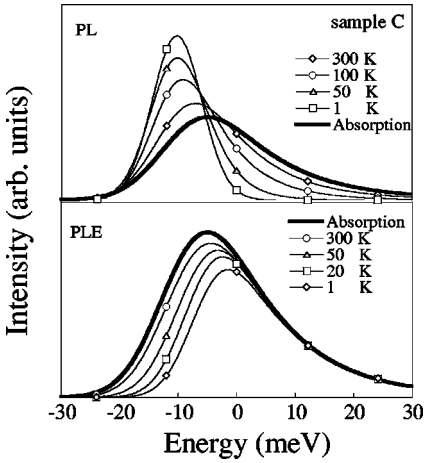

FIG. 8. Simulation results for parameters corresponding to sample C. Analytical fits to the histograms obtained for luminescence (PL, thin lines in upper panel), absorption (thick line in both panels), and excitation spectra (PLE, thin lines in lower panel) are reported. The normal behavior of the Stokes shift SS is clearly seen in the maximum positions, the anomalous behavior reported in Fig. 7 is not resolved here. The trend of the line width manifests itself more clearly in the heights of the normalized peaks. PLE curves are scaled with an (almost) temperature-independent factor to coincide with the high energy behavior of absorption. The blueshift SS′ clearly increases with falling temperature.

are the weighted sum of the emission intensities over all the detection energies, of course, excluding the resonant emission (as done in PLE experiments). For decreasing temperature, the HHE PL band becomes more symmetric and exhibits an increasing red shift with respect to the absorption band whose nonmonotonic dependence on T has been reported in detail in Fig. 7. The HHE PLE band, instead, is highly asymmetric at all temperatures. Moreover, for decreasing temperatures, it exhibits an increasing blueshift SS′ with respect to the absorption band. This shift is related to the presence of an effective mobility edge that leads to a suppression of the exciton relaxation into low-energy states.[25]

This blueshift of the PLE spectra is considerably smaller than the redshift of the PL spectra and depends on temperature as well as on detection energy (qualitatively, a detection energy in PLE deep in the tail of the density of states leads to a smaller SS′). The finite, although small, value of SS′ at low temperatures distinguishes, therefore, the definition of SS in terms of the difference between the peak energies of the HHE in the absorption and PL spectra from its operative definition used here, and in most of the literature for strained QW's. The latter definition, in fact, relies on the assumption that peak energies of PLE and absorption spectra coincide at all temperatures.

In order to experimentally and quantitatively verify the theoretical prediction of a finite value for SS′, at least at low T, we need a procedure for its estimates from the PLE data. As already mentioned, an estimate of the absorption spectra in strained QW's is intrinsically quite unreliable. Therefore, we estimate SS′ for the two samples, C and D, where the value of SS′ is expected to be higher, on the grounds of a somewhat crude approximation. We extrapolate the value of the absorption peak energy at low T from the fit of the temperature dependence measured at high T's ($T \gtrsim 60$ K) for the

TABLE III. Best values of the parameters E_b, a_b, and Θ entering the fit of the dependence on T of the HHE peak in the PLE spectra, for the most disordered $In_xGa_{1-x}As$ samples C and D. The parameters fitting the dependence on T of the GaAs energy gap are taken from Ref. 27 and are reported in the last row with the corresponding estimated uncertainties.

Sample	E_b (eV)	a_b (meV)	Θ (K)
C	1.425	54	210
D	1.485	54	240
GaAs bulk	1.571 ± 0.023	57 ± 29	240 ± 102

PLE HHE peak energy. In fact SS′ (and SS) vanishes and the PLE spectrum reproduces well the absorption spectrum at T's high enough that carriers freely relax and thermalize through the full density of states, as previously discussed. The PLE energy peak curves are then expected to follow the high-temperature dependence of the InGaAs band gap.[26] This dependence is assumed to be given by

$$E(T)=E_b-a_b\left(1+\frac{2}{e^{\Theta/T}-1}\right), \tag{3}$$

namely, to be determined by the Bose-Einstein statistical factor for phonons with an average frequency Θ. This formula well describes the dependence on T of the GaAs energy gap.[27] The values of the three fitting parameters Θ, E_b, and a_b, which are allowed to vary in order to account for different thicknesses and indium concentrations, are reported in Table III. Within the uncertainties, the a_b and Θ values are equal to those estimated in GaAs and reported in the last row of the table. The experimental data and their best fits are given in Fig. 9 by triangles and full lines, respectively. At low Ts, the data exibit a small but clear deviation from the reference curves, faster in the most disordered sample D with broader PLE and PL exciton bands.

SS′ values at 10 K are reported in Table IV for samples C and D. In the other two samples A and B, SS′ is $\approx$1 meV. In the same table are also summarized the values for all other parameters related to disorder, as estimated from the experiment and from the theoretical simulations. As already discussed, the quantitative agreement with the experiment is fair for $R=0.1$, it improves for $R=1$, for all parameters except

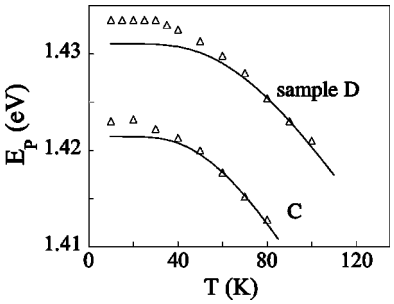

FIG. 9. Comparison between the temperature dependence of the PLE peak energies for the different $In_xGa_{1-x}As$ samples (triangles) and the corresponding absorption peaks (full lines), as derived by fitting Eq. (3) to the high-temperature data. For comparison's sake, both PLE peak energies and absorption peaks for sample C have been shifted by 50 meV toward higher energies.

TABLE IV. Theoretical and experimental estimates of different parameters characterizing the emission spectra of samples C and D, the two more disordered $In_xGa_{1-x}As$ samples investigated here: 10 K values of the blueshift SS′, of the Stokes shift SS, and of W', the FWHM of the PL HHE band. Both the experimental and theoretical estimates of SS have been obtained as the difference between the peak energies of the HHE band in PL and PLE spectra. The values of the temperature T_M for which SS is maximum and of the temperature T_m for which W' is minimum are also reported. Theoretical estimates have been obtained for $R=D_v/D_c=1$ (in brackets for $R=0.1$). Experimental estimates have been obtained from spectra taken at the lowest excitation power density (50 W cm^{-2}).

Sample		SS′ (meV)	SS (meV)	T_M (K)	T_m (K)	W' (meV)
C	exp	1.7 ± 2	18 ± 2	22 ± 5	10 ± 5	9.3 ± 1
C	sim	3.5 (5.0)	9.0 (7.0)	15 (10)	15 (12)	12.8 (13.8)
D	exp	2.5 ± 2	23.5 ± 2	20 ± 5	15 ± 5	11.9 ± 1
D	sim	6.0 (5.0)	15.0 (9.5)	15 (5)	20 (15)	19.4 (21.4)

T_m. In particular, SS′ increases with disorder as expected, although it results smaller than theoretically predicted. A better agreement is found if experiment and simulations are compared by looking directly at the shift of the PL with respect to the PLE spectra, without introducing the intermediate step of absorption.

The discrepancy between experimental and theoretical estimates of SS′ may be justified by the fact that both determinations are delicate. In fact, while the experiments have been analyzed by fitting the peaks with Gaussian, different options are available for the discussions of the numerical results. Each option has its specific drawback because the underlying optical density or absorption is intrinsically asymmetrical with a rather long tail to the high-energy side.

PLE spectra are even more asymmetrical, as they share the absorption's high-energy tail and fall rather rapidly below the effective relaxation mobility edge, see Fig. 8 (lower panel) and Fig. 1 (experiment). Absorption and PLE spectra can be fitted well by the product of an error function and an exponential. The former describes the rapid fall on the low-energy side, whereas the latter describes the high-energy tail. The form of the high-energy tail can be understood on the ground of second order perturbation theory and reflects the Fourier transform of the square of the excitons relative wave function. In contrast, low-temperature PL and resonant secondary emission (i.e., light emitted at the excitation frequency) can be fitted typically by Gaussians with good accuracy, see Fig. 8 (upper panel) and Fig. 1 (experiment).

A Stokes shift SS′ defined in terms of an average energy exhibits a smaller dependence on temperature than that defined, e.g., in terms of the position of the low-energy half maximum. This feature and the uncertainty in the fit of the absorption position are, in our opinion, the primary reasons for having found experimental values for SS′ systematically smaller than those obtained in the simulation.

In conclusion of this section, it might be useful to distinguish two conceptually different aspects of incomplete relaxation, both contributing to SS′ and the nonmonotonic behavior of SS. First, we can think of the scattering becoming slow at low temperatures and comparable to the radiative lifetime.

For broad lines and acoustic phonons, which carry away only a limited amount of energy at a time, it takes several scattering events to relax to thermal energies and the exciton population might fail to reach a thermal distribution. In such a scenario, the temperature-dependent SS depends very sensitively on the scattering rates. The second, somehow opposite limit is the picture of excitons relaxing into well separated local minima with very small transfer rates between them. In such a picture, uncertainties in the prefactors of the scattering strengths are almost irrelevant for the qualitative features of SS and SS′, as the rates are assumed to become exponentially small in the low-energy tail. The differences of the qualitative behavior of SS and PL-FWHM from sample to sample, seen both in the experiment and in the simulation, and the dependence of the simulation results on the input parameters, in particular the deformation potentials, point to the fact that the InGaAs system is in between these two scenarios. In particular, both pictures allow us to understand the occurrence of a blueshift SS′, with a weaker dependence on the detection energy of SS′ in the mobility edge picture.

IV. CONCLUSIONS

Since the lifetime of excitons is finite, the competition between the radiative exciton decay and the exciton energy relaxation due to phonon scattering in a disordered potential leads to an incomplete relaxation of excitons, in particular at low temperatures. This gives rise to the prediction of a series of features in the optical response of a disordered system that are ''anomalous'' with respect to those characteristic of thermalized excitons. These ''anomalous'' features, including some subtle ones, have all been experimentally observed by PL and PLE performed in a number of $In_xGa_{1-x}As$ QW's grown by MBE or MOCVD. These samples differ for the indium concentration and the well thickness, as well as for degree of disorder, and are all characterized by fluctuations in the potential energy comparable with thermal energies between 4.2 and 60 K. All the anomalous features here reported have been shown to depend on the sample degree of disorder. Two different scenarios for incomplete carrier relaxation have been discussed which both account for the ''anomalous'' behavior of SS and SS′. The dependence of the simulation results on the input parameters, in particular the deformation potentials, suggests that the InGaAs system is in-between these two scenarios.

ACKNOWLEDGMENTS

We thank A. Siarkos for the $\mathbf{k}\cdot\mathbf{p}$ calculation of single-particle bands, S. Franchi and A. Bosacchi for having provided the MBE samples, and R. Cingolani for having provided the MOCVD sample. It is also a pleasure to acknowledge F. Martelli for useful discussions and suggestions. This work has been partially supported by the project MADESS-CNR, by the MURST, and by DFG within Sfb296.

[1] M. Gurioli, A. Vinattieri, J. Martinez-Pastor, and M. Colocci, Phys. Rev. B **50**, 11 817 (1994).

[2] F. Yang, M. Wilkinson, E. J. Austin, and K. P. O'Donnell, Phys. Rev. Lett. **70**, 323 (1993).

[3] E. Runge and R. Zimmermann, Adv. Solid State Phys. **38**, 251 (1998); Phys. Status Solidi A **164**, 511 (1997).

[4] R. Zimmermann and E. Runge, J. Lumin. **60-61**, 320 (1994).

[5] A. Polimeni, A. Patané, M. Grassi Alessi, M. Capizzi, F. Martelli, A. Bosacchi, and S. Franchi, Phys. Rev. B **54**, 16 389 (1996).

[6] M. S. Skolnick, P. R. Tapster, S. J. Bass, A. D. Pitt, N. Apsley, and S. P. Aldred, Semicond. Sci. Technol. **1**, 29 (1986), and references therein.

[7] P. G. Eliseev, P. Perlin, J. Lee, and M. Osinski, Appl. Phys. Lett. **71**, 569 (1997); a non-monotonic Stokes shift has been seen in the InGaN/GaN system also by Igor Kukovsky (private communication).

[8] S. T. Davey, E. G. Scott, B. Wakefield, and G. J. Davies, Semicond. Sci. Technol. **3**, 365 (1988).

[9] E. M. Daly, T. J. Glynn, J. D. Lambkin, L. Considine, and S. Walsh, Phys. Rev. B **52**, 4696 (1995).

[10] W. Braun, L. V. Kulik, T. Baars, M. Bayer, and A. Forchel, Phys. Rev. B **57**, 7196 (1998).

[11] Robert Klann (unpublished).

[12] A. Patané, M. Grassi Alessi, F. Intonti, A. Polimeni, M. Capizzi, F. Martelli, M. Geddo, A. Bosacchi, and S. Franchi, Phys. Status Solidi A **164**, 493 (1997).

[13] A. Polimeni, A. Patané, M. Henini, L. Eaves, and P. C. Main, Phys. Rev. B **59**, 5064 (1999).

[14] L. E. Golub, S. V. Ivanov, E. L. Ivchenko, T. V. Shubina, A. A. Toropov, J. P. Bergman, G. R. Pozina, B. Monemar, and M. Willander, Phys. Status Solidi B **205**, 203 (1998).

[15] S. D. Baranovskii, R. Eichmann, and P. Thomas, Phys. Rev. B **58**, 13 081 (1998).

[16] *Properties of Lattice-Matched and Strained Indium Gallium Arsenide*, EMIS Datareviews Series No. 8, edited by P. Bhattacharya (IEE, London, 1993).

[17] D. B. Tran Thoai, R. Zimmermann, M. Grundmann, and D. Bimberg, Phys. Rev. B **42**, 5906 (1990).

[18] P. Yu and M. Cardona, *Fundamentals of Semiconductors* (Springer, Berlin, 1996).

[19] Roland Winkler, Ph.D. thesis, Regensburg, 1994.

[20] It should be mentioned that monolayer splittings of the exciton have never been observed in InGaAs/GaAs QW's, since in this material well width fluctuates in the QW plane on a characteristic scale smaller than the exciton Bohr radius; see Ref. 21, and references therein.

[21] F. Martelli, A. Polimeni, A. Patané, M. Capizzi, P. Borri, M. Gurioli, M. Colocci, A. Bosacchi, and S. Franchi, Phys. Rev. B **53**, 7421 (1996).

[22] The growth of $In_xGa_{1-x}As$ on GaAs is expected to follow the Stranski-Krastanov mode until the strain induced by the mismatch between the two lattice parameters is partially released by the self-aggregation of three-dimensional islands—the so-called quantum dots (QD's)—for QW thicknesses L exceeding a critical value L_c. In all samples measured here, L is below L_c. Moreover, the line shape of the PL and PLE bands, as well as their dependence on temperature and power, rule out the presence of well defined, stand alone QD's. Nevertheless, the high

degree of interface disorder could lead to the formation of islands which behave as precursors of QD's, see Ref. 23, and may strongly localize excitons.

[23] C. Priester and M. Lannoo, Phys. Rev. Lett. **75**, 93 (1995).

[24] The minor differences in the heavy- and light-hole exciton peak energies observed in PLE in the nominally identical samples A and D are likely due to deviations of x and L from the nominal values.

[25] U. Jahn, M. Ramsteiner, R. Hey, T. Grahn, E. Runge, and R. Zimmermann, Phys. Rev. B **56**, R4387 (1998).

[26] The above procedure is made possible by the absence of substantial changes in the PLE HHE line shape for detection energies consistently taken on the low energy tail of the PL band.

[27] P. Lautenschlager, M. Garriga, S. Logothetidis, and M. Cardona, Phys. Rev. B **31**, 2163 (1985).